Journal of Cerebral Blood Flow & Metabolism (2012) 32, 676–684

www.jcbfm.com

The utility of ^{11}C-arachidonate PET to study *in vivo* dopaminergic neurotransmission in humans

Madhav Thambisetty[1], Kathy A Gallardo[2], Jeih-San Liow[3], Lori L Beason-Held[4], John C Umhau[5], Abesh K Bhattacharjee[1], Margaret Der[6], Peter Herscovitch[6], Judith L Rapoport[2] and Stanley I Rapoport[1]

[1]*Brain Physiology and Metabolism Section, National Institute on Aging, National Institutes of Health, Bethesda, Maryland, USA;* [2]*Child Psychiatry Branch, National Institute of Mental Health (NIMH), National Institutes of Health, Bethesda, Maryland, USA;* [3]*Molecular Imaging Branch, National Institute of Mental Health (NIMH), National Institutes of Health, Bethesda, Maryland, USA;* [4]*Laboratory of Behavioral Neuroscience, National Institute on Aging, National Institutes of Health, Bethesda, Maryland, USA;* [5]*Laboratory of Clinical and Translational Studies, National Institute of Alcohol Abuse and Alcoholism, National Institutes of Health, Bethesda, Maryland, USA;* [6]*PET Department, Clinical Center, National Institutes of Health, Bethesda, Maryland, USA*

We developed a novel method to study dopaminergic neurotransmission using positron emission tomography (PET) with [1-^{11}C]arachidonic acid ([1-^{11}C]AA). Previous preclinical studies have shown the utility of [1-^{11}C]AA as a marker of signal transduction coupled to cytosolic phospholipase A_2 ($cPLA_2$). Using [1-^{11}C]AA and [^{15}O]water PET, we measured regional incorporation coefficients K* for AA and regional cerebral blood flow (rCBF), respectively, in healthy male volunteers given the D_1/D_2 agonist (10 or 20 μg/kg subcutaneous) apomorphine. We confirmed a robust central dopaminergic response to apomorphine by observing significant increases in the serum concentration of growth hormone. We observed significant increases, as well as decreases in K* and increases in rCBF in response to apomorphine. These changes remained significant after covarying for handedness and apomorphine dosage. The magnitude of increases in K* was lower than those in our previous animal experiments, likely reflecting the smaller dose of apomorphine used in the current human study. Changes in K* may reflect neuronal signaling downstream of activated D_2-like receptors coupled to $cPLA_2$. Changes in rCBF are consistent with previous studies showing net functional effects of D_1/D_2 activation. [1-^{11}C]AA PET may be useful for studying disturbances of dopaminergic neurotransmission in conditions such as Parkinson's disease and schizophrenia.
Journal of Cerebral Blood Flow & Metabolism (2012) **32,** 676–684; doi:10.1038/jcbfm.2011.171; published online 14 December 2011

Keywords: apomorphine; $cPLA_2$; D_1/D_2 receptors; [1-^{11}C]arachidonate PET; regional cerebral blood flow

Introduction

Neuroimaging studies of dopaminergic function in the human brain predominantly rely upon the demonstration of receptor localization or measurement of dopamine synthesis/transport (Cropley *et al*, 2006; Elsinga *et al*, 2006; Volkow *et al*, 2009). These methods have helped to understand synaptic mechanisms relevant to dopaminergic neurotransmission in healthy subjects and in disease states. However, these approaches do not provide information on dopamine receptor-initiated signaling events in the brain, which might be useful for understanding physiologic mechanisms underlying normal dopamine function, as well as perturbations in disease states such as schizophrenia and Parkinson's disease (Brooks and Piccini, 2006; Hirvonen and Hietala, 2011; Dolan *et al*, 1995). The ability to study specific *in vivo* signal transduction mechanisms underlying dopamine neurotransmission might be useful in the development of pharmacological manipulations that target disease-specific abnormalities in dopamine pathways (Nikolaus *et al*, 2007).

We have reported on a quantitative autoradiography method in unanesthetized rodents designed to study signal transduction through dopaminergic D_2-like receptors in response to a pharmacological

Correspondence: M Thambisetty, Brain Physiology and Metabolism Section, National Institute on Aging (NIA), Room 1S-126, Bluiding-9, 9000 Rockville Pike, Bethesda, Maryland 20892, USA.
E-mail: thambisettym@mail.nih.gov
This study was supported by the Intramural Program of the National Institute of Mental Health, National Institute on Aging, National Institute of Neurological Disorders and Stroke, and National Institute of Alcohol Abuse and Alcoholism.
Received 20 June 2011; revised 29 September 2011; accepted 30 September 2011; published online 14 December 2011

challenge with apomorphine, a D_1/D_2 receptor agonist and have shown that this signaling can be prevented by pretreatment with the D_2 receptor antagonist, raclopride (Bhattacharjee *et al*, 2005, 2006, 2007, 2008*a*, *b*; Hayakawa *et al*, 1998, 2001). This method takes advantage of the coupling of D_2 receptors through a G-protein mechanism to Ca^{2+}-dependent cytosolic phospholipase A_2 ($cPLA_2$), which upon receptor activation, selectively releases the polyunsaturated fatty acid, arachidonic acid (AA, 20:4n-6) from membrane phospholipids (Clark *et al*, 1991; Rapoport, 2001, 2003; Vial and Piomelli, 1995). After $cPLA_2$ activation, unesterified AA in the plasma is rapidly taken up by the brain to replace the AA that was released from membrane phospholipids. This replacement can be quantified as an incorporation coefficient K* for AA, equal to brain radioactivity divided by integrated plasma radioactivity owing to intravenously injected radiolabeled AA (Robinson *et al*, 1992). The incorporation coefficient K* is proportional to $cPLA_2$-mediated release of AA from synaptic membrane phospholipids and is independent of changes in regional cerebral blood flow (rCBF) (Chang *et al*, 1997; Robinson *et al*, 1992), thereby making it a valid neuroimaging marker of $cPLA_2$ activation during changes in baseline functional activity or neuroreceptor-mediated signal transduction involving AA.

We have extended this method in human subjects, using positron emission tomography (PET), to quantitatively study brain signal transduction involving AA, at rest and after visual stimulation (Esposito *et al*, 2007; Giovacchini *et al*, 2002, 2004). In this study, we used PET with [1-^{11}C]AA to test the hypothesis, based in part on preclinical imaging after apomorphine (Bhattacharjee *et al*, 2008*b*), that regional changes in the incorporation of AA in the brain can be detected after a pharmacological challenge with apomorphine. Apomorphine is a mixed D_1/D_2 receptor agonist the affinity of which for D_2-like (D_2, D_3, D_4) receptors is 10 times higher than that for D_1-like (D_1 and D_5) receptors (Scarselli *et al*, 2001). However, because D_1 receptors are not coupled to $cPLA_2$ activation, apomorphine is believed to release AA from membrane phospholipids solely through a D_2-like coupled mechanism (Bhattacharjee *et al*, 2005, 2006, 2008*b*; Nilsson *et al*, 1998; Vial and Piomelli, 1995).

Our secondary aim was to identify apomorphine-induced changes in rCBF, as a measure of changes in functional activity, using ^{15}O-water PET. A previous PET study in healthy volunteers scanned twice before and after 10 μg/kg subcutaneous apomorphine, while performing a cognitive task, revealed that apomorphine increased rCBF in the anterior cingulate, ventral motor cortex, and the dorsolateral prefrontal cortex, while decreasing rCBF in the retrosplenial cingulate region (Kapur *et al*, 1994). These regions are believed to form a functional network modulated by the dopaminergic system. Similarly, in a study on normal volunteers, 10 μg/kg apomorphine compared with saline injection increased rCBF in the anterior cingulate and prefrontal cortices without any observed reductions in rCBF (Grasby *et al*, 1993). In another study, schizophrenic patients performing a cognitive task displayed significantly enhanced rCBF in the anterior cingulate cortex relative to controls after pharmacological challenge with apomorphine (Dolan *et al*, 1995).

Taken together with these previous findings, we reasoned that measuring AA incorporation and rCBF in response to apomorphine in healthy volunteers during a 'resting state' would delineate the regional anatomic distribution of signal transduction coupled to $cPLA_2$ through D_2-like receptors, as well as neuronal activity, initiated by stimulation of D_1/D_2 receptors.

Materials and methods

Participants

Research participants in this study were recruited as part of a clinical protocol (protocol number: 06-M-0246) approved by the Combined Neuroscience Institutional Review Board and by the Radiation Safety Committee of the National Institutes of Health (NIH). Subjects were healthy adult male volunteers ($N = 12$, age range 23 to 52 years; mean 32 years) without a significant history of psychiatric illness. All participants provided written informed consent before enrolment in this study. Nine of the participants were right handed, whereas three were left handed. Exclusion criteria included current history of smoking, use of recreational drugs, hypertension, significant neurologic illness, head trauma with loss of consciousness, metabolic, endocrine, or connective tissue disease, abnormal renal, liver, or pulmonary function, blood dyscrasias, malignancy, stimulant pharmacotherapy within 1 month of the study, or any history of use of antipsychotic medication. Participants were instructed not to use nonsteroidal antiinflammatory drugs (1 week) and to avoid alcohol (48 hours) or caffeine (24 hours) before the PET scan. Participants were admitted to the NIH Clinical Center the day before the PET study and were premedicated with trimethobenzamide (300 mg p.o. q.i.d.) to prevent apomorphine-induced nausea (Bowron, 2004).

Positron Emission Tomography Scanning

Here, [1-^{11}C]AA was synthesized as reported previously (Chang *et al*, 1997; Channing *et al*, 1992). The tracer was 97.6% pure on high-performance liquid chromatography, and its specific activity exceeded 3,700MBq (100mCi)/μmol. On the day of PET imaging, an indwelling radial artery catheter was inserted under local anesthesia in the nondominant hand and an ante-cubital venous catheter inserted in the contralateral arm. The subject's head was secured in a thermoplastic face mask fixed to the scanner bed. Scanning was performed using an Advance Tomograph (GE Healthcare, Waukesha, WI, USA), which acquires 35 simultaneous slices with 4.25-mm separation

and has in-plane and axial resolutions of 6 to 7 mm. Scans were performed parallel to the orbitomeatal line and were conducted in a quiet, dimly lit room, with the subject's eyes open and ears unoccluded.

For each subject, two separate PET scans were acquired on the same day with an interval of 1.5 hours between each session. In the first session, a transmission scan was initially performed for attenuation correction. After the transmission scan, ~0.15 mL of saline vehicle was injected subcutaneously. Three minutes later, 370MBq (10mCi) of ^{15}O-water was injected as an intravenous bolus. A 60-second scan in the three-dimensional mode started automatically when the bolus reached the brain, detected by a threshold of count increase. Concurrent to PET scanning, arterial input function was measured continuously using an automated blood counter (Herscovitch *et al*, 1983). To quantify regional values of K* for AA, 15 minutes after the ^{15}O-water injection, 920 ± 115MBq (24.9 ± 3.1mCi) of 1-^{11}C-AA was infused intravenously for 1 minutes at a constant rate. Serial dynamic three-dimensional scans (30 seconds to 5 minutes) were performed for 1 hour. Radial artery blood (1 to 3 mL) was sampled manually at fixed times, and radioactivity in whole blood and plasma measured using a γ-counter. The second PET session was identical to the first but was performed after injecting apomorphine (4 subjects with 20 μg/kg subcutaneous, 8 subjects with 10 μg/kg subcutaneous; see the 'Results' section) in place of saline vehicle after a second transmission scan. Subjects were allowed to get off the bed in between the two scanning sessions.

Coregistration to Magnetic Resonance Images

For each subject, the original PET image of 1-^{11}C-AA injection was registered to the ^{15}O-water image to correct for motion between the two scans, using a six-parameter transformation and a mutual information cost function (Giovacchini *et al*, 2004; Jenkinson and Smith, 2001). The [^{15}O]water and magnetic resonance imaging images of the individual subject were then coregistered using the same six-parameter algorithm. The product of the two transformation matrices was used to bring the dynamic image of [1-^{11}C]AA into the magnetic resonance imaging space where correction for partial volume effect (PVE) and modeling took place. Partial volume correction was performed by implementing the magnetic resonance imaging-based three-compartment model described by Muller-Gartner *et al* (1992). Details of procedures adopted for motion correction of images, generation of plasma time–activity curves, and partial volume correction have been described previously (Giovacchini *et al*, 2002, 2004).

Modeling

On a pixel-by-pixel basis, rCBF images were generated using the [^{15}O]water scan and continuous arterial blood samples. Parametric images of K* for AA (incorporation coefficient of plasma AA into the brain tissue, μL/min per cm^3 of the brain) and of V_b (cerebral blood volume, (mL of blood)/(cm^3 of brain)) were generated using dynamic images of [1-^{11}C]AA and arterial blood input, by the following equation (Giovacchini *et al*, 2002),

$$C_i(t-\Delta t) = V_b C_b(t) + K * \int_0^t C_p(s)\mathrm{d}s + C_{CO_2}(t)$$

where $C_i(t)$, $C_b(t)$, and $C_p(t)$ are pixel, whole-blood, and plasma 1-^{11}C-AA time–activity curves, respectively; $C_{CO_2}(t)$ is the predicted brain tissue concentration of [^{11}C]CO_2; and Δt is the delay between the brain and blood curves derived using a tri-exponential function. Tissue [^{11}C]CO_2 concentration was computed for each subject by measuring plasma [^{11}C]CO_2 concentration and applying a one-tissue compartment model with published values of the gray matter influx rate constant (K_1) and the distribution volume for CO_2 (Brooks *et al*, 1984). Calculations were applied to the reconstructed PET with correction for PVE (Giovacchini *et al*, 2002; Ibanez *et al*, 1998).

Positron Emission Tomography Data Analysis

The rCBF and K* images were realigned and spatially normalized into standard stereotactic space and smoothed to full-width at half-maximum of $10 \times 10 \times 10$ mm^3 in the x, y, and z planes. The image data were analyzed using Statistical Parametric Mapping (SPM5; Wellcome Department of Cognitive Neurology, London, UK). To examine the differences in rCBF and K* between the saline and apomorphine conditions, whole-brain voxel-by-voxel group differences between the two conditions were performed. Baseline age was included as a covariate. In a secondary analysis, we also included handedness (right or left) and apomorphine dose (i.e., 10 or 20 μg/kg subcutaneous) as covariates. To reduce the risk of type-I error caused by multiple comparisons, significant effects for each contrast are reported at a statistical threshold of $P \leqslant 0.005$ in regions with a spatial extent >20 voxels. Furthermore, only changes in K* or rCBF that exceeded ± 2% from baseline are reported.

Measurement of Serum Growth Hormone

Arterial blood samples (2 mL) were collected at baseline on the morning of the PET scan (G0), as well as 30 and 60 minutes after saline (G1 and G2, respectively) and apomorphine (G3 and G4, respectively) injections, for measurement of serum growth (GH) hormone concentrations. Serum samples were assayed for GH concentration using a chemiluminiscent immunometric assay (IMMULITE 2500, Siemens USA, Deerfield, IL, USA) as per the manufacturer's instructions.

Results

Apomorphine Induced Changes in Brain Incorporation Coefficient K* of Arachidonic Acid

After pharmacological challenge with apomorphine, we observed significant increases in the regional

incorporation coefficients K* of AA in distinct brain regions relative to the saline condition. Affected regions included the left superior medial frontal gyrus (Brodmann area (BA) 6), right superior frontal gyrus (BA 8), right superior temporal gyrus (BA 38), right precentral gyrus/motor cortex (BA 4), right fusiform gyrus (BA 20), brainstem, and the right cerebellar hemisphere (Figure 1, Table 1).

Apomorphine-induced decreases in K* for AA were observed in the left superior frontal gyrus (BA 6), right precentral gyrus/motor cortex (BA 4), right paracentral lobule (BA 5), right inferior parietal lobule (BA 40), left inferior frontal gyrus (BA 44), left hippocampus, left middle frontal gyrus (BA 46), right anterior cingulate gyrus (BA 32), right superior frontal gyrus (BA 10), right fusiform gyrus (BA 20), right superior temporal gyrus (BA 38), and regions within bilateral cerebellar hemispheres (Figure 1, Table 1). The observed changes in apomorphine-induced incorporation coefficients K* of AA

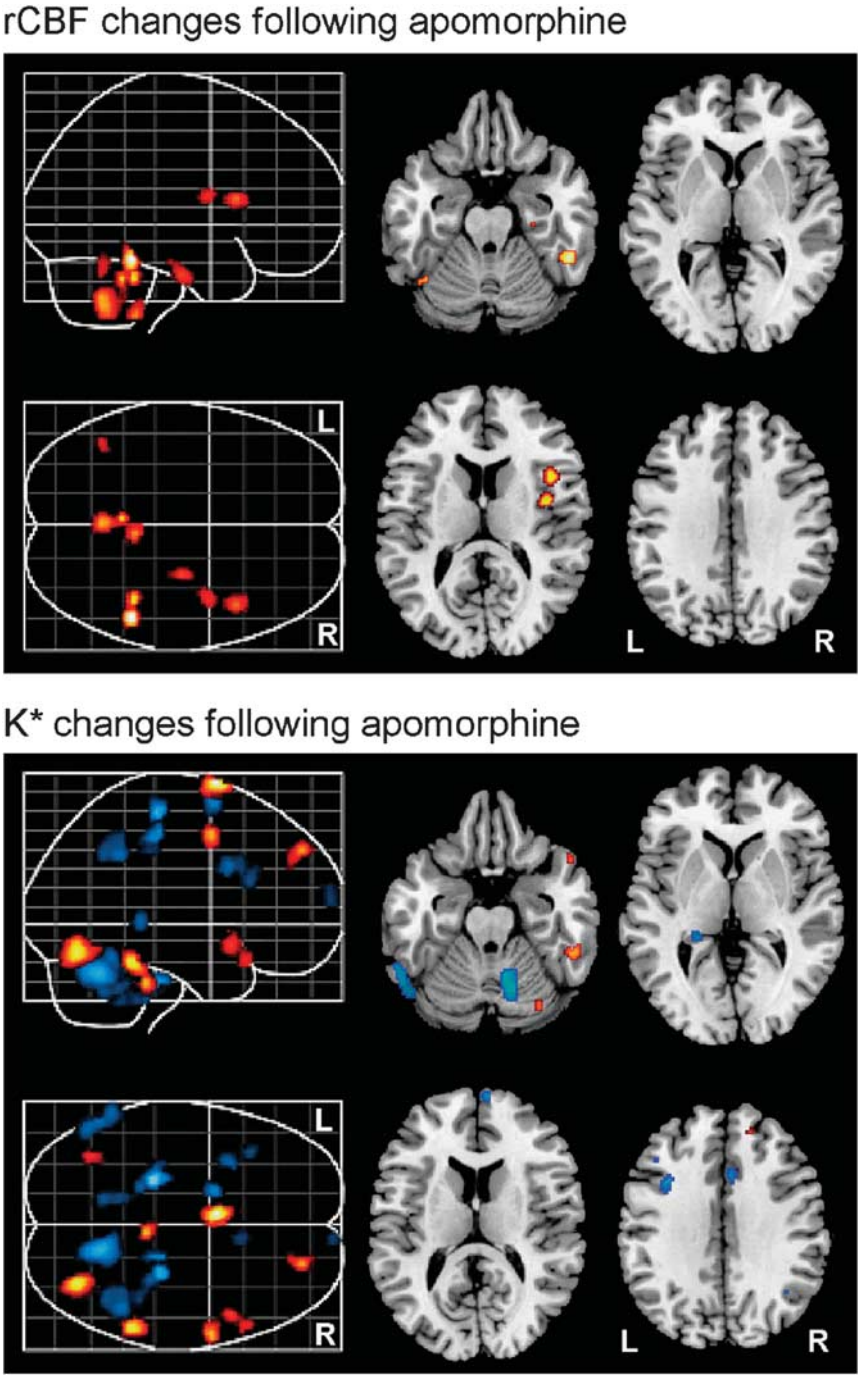

Figure 1 Representative differences in rCBF (top) and K* (bottom) in the brain after apomorphine challenge (relative to saline vehicle). Red and blue regions indicate significant increases and decreases, respectively. rCBF, regional cerebral blood flow.

Table 1 Local maxima within areas of significant differences in incorporation coefficient K* for arachidonic acid after apomorphine challenge

Region	*Side*	X	Y	Z	t-*value*	P *uncorrected*	*Tissue volume (mL)*	*Change from baseline %*	μL/*min per cm*^{3}	
									K before APO (SD)*	*K* after APO (SD)*
Decrease in K after apomorphine*										
Cerebellum	L	−26	−30	−34	4.99	<0.001	142	9.26	61.51 (4.43)	55.81 (4.35)
Cerebellum	R	12	−60	−26	4.62	<0.001	732	10.12	74.68 (5.46)	67.12 (4.22)
Primary motor cortex (4)	R	24	−28	60	4.56	<0.001	106	9.79	65.09 (4.10)	58.72 (4.83)
Paracentral lobule (5)	R	16	−26	48	4.08	<0.001	74	9.70	63.70 (5.60)	57.52 (5.66)
Superior frontal gyrus (6)	L	−20	4	66	3.98	<0.001	142	7.94	76.03 (7.01)	69.99 (6.09)
Inferior parietal lobule (40)	R	42	−48	38	3.69	<0.001	302	8.45	65.68 (6.35)	60.13 (5.79)
Cerebellum	L	−56	−58	−26	3.68	<0.001	374	8.50	69.85 (6.84)	63.91 (6.59)
Inferior frontal gyrus (44)	L	−34	12	32	3.61	<0.001	70	9.15	65.86 (8.55)	59.83 (4.63)
Hippocampus	L	−22	−36	0	3.58	0.001	64	7.12	72.06 (6.82)	66.93 (5.63)
Cerebellum	R	28	−32	−38	3.53	0.001	154	9.49	62.49 (6.60)	56.56 (4.00)
Cerebellum	L	−16	−56	−36	3.46	0.001	114	8.79	62.05 (4.49)	56.59 (3.59)
Middle frontal gyrus (46)	L	−40	22	24	3.30	0.001	68	6.86	72.19 (6.24)	67.24 (4.47)
Anterior cingulate gyrus (32)	R	6	16	32	3.16	0.002	56	9.04	66.99 (3.67)	60.93 (4.87)
Superior frontal gyrus (10)	R	6	66	12	3.13	0.002	54	6.94	70.35 (4.61)	65.47 (3.58)
Increase in K after apomorphine*										
Superior medial frontal gyrus (6)	L	−6	4	76	4.28	<0.001	158	6.41	64.82 (5.33)	69.26 (3.75)
Cerebellum	R	30	−70	−16	3.98	<0.001	318	5.21	72.96 (7.11)	76.97 (4.40)
Fusiform gyrus (20)	R	52	−42	−20	3.95	<0.001	134	4.70	63.49 (6.13)	66.61 (5.98)
Brain stem	R	4	−34	−32	3.60	0.001	64	6.05	53.98 (4.17)	57.45 (3.25)
Primary motor cortex (4)	R	56	2	50	3.60	0.001	128	4.06	71.80 (3.12)	74.83 (3.27)
Superior frontal gyrus (8)	R	20	50	40	3.55	0.001	82	4.02	67.28 (4.44)	70.10 (6.11)
Superior temporal gyrus (38)	R	46	12	−12	3.28	0.001	68	4.48	63.65 (3.85)	66.64 (5.01)
Fusiform gyrus (37)	R	−36	−62	−14	3.17	0.002	40	3.50	63.29 (3.03)	65.59 (5.70)
Superior temporal gyrus (38)	R	52	20	−20	3.11	0.002	40	5.49	67.56 (5.63)	71.48 (6.82)

APO, apomorphine.
Coordinates for peak voxels are in stereotactic space and Brodmann numbers are in parentheses.

Table 2 Local maxima within areas of significant differences in rCBF after apomorphine challenge

Region	*Side*	X	Y	Z	t-*value*	P *uncorrected*	*Tissue volume (mL)*	*Change from baseline %*	*mL/100g per min*	
									rCBF before APO (SD)	*rCBF after APO (SD)*
Increase in rCBF after apomorphine										
Fusiform gyrus (20)	R	52	−44	−20	4.10	<0.001	220	12.58	50.03 (4.10)	57.23 (3.96)
Cerebellum	L	−4	−48	−30	3.53	0.001	318	12.43	45.69 (4.22)	51.82 (4.98)
Brainstem	R	4	−40	−50	3.40	0.001	82	14.94	48.09 (5.46)	56.54 (4.39)
Insula	R	44	14	12	3.31	0.001	120	12.72	55.61 (6.17)	63.72 (7.18)
Parahippocampal gyrus (35)	R	28	−16	−28	3.22	0.001	66	12.97	48.99 (3.39)	56.30 (4.98)
Insula	R	40	−2	14	3.11	0.002	74	11.67	49.27 (3.60)	55.78 (4.74)
Cerebellum	L	−42	−58	−24	2.98	0.003	48	11.45	62.66 (3.57)	70.76 (4.24)

APO, apomorphine; rCBF, regional cerebral blood flow.
Coordinates for peak voxels are in stereotactic space and Brodmann numbers are in parentheses.

remained significant even after covarying for subject handedness and apomorphine dosage.

Apomorphine Induced Changes in Regional Cerebral Blood Flow

We observed significant increases in rCBF after administration of apomorphine relative to the saline condition, in the right fusiform gyrus (BA 20), right parahippocampal gyrus (BA 35), right insula, as well as in bilateral cerebellar hemispheres (Figure 1, Table 2). The observed changes in apomorphine-induced rCBF remained significant even after covarying for subject handedness and apomorphine dosage.

Serum Growth Hormone Concentration

The mean serum GH concentration at baseline (G0) was 0.16 ng/mL (range < 0.1 to 0.6 ng/mL). The mean serum GH concentrations after 30 minutes (G1) and 60 minutes (G2) after injection of saline vehicle were 0.3 ng/mL (range < 0.1 to 0.9 ng/mL) and 2.9 ng/mL

Table 3 Mean serum growth hormone (GH) concentrations measured at baseline (G0), 30 and 60 minutes following saline (G1 and G2, respectively) and apomorphine (G3 and G4, respectively)

Baseline; (G0) ng/mL	*30 minutes after saline injection (G1) ng/mL*	*60 minutes after saline injection (G2) ng/mL*	*30 minutes after apomorphine injection (G3) ng/mL*	*60 minutes after apomorphine injection (G4) ng/mL*
0.16 (<0.1–0.6)	0.3 (<0.1–0.9)	2.9 (0.1–19.1)	13.4 (0.1–53.8)	11.9 (2.1–37.0)

Numbers in parentheses represent the range (minimum–maximum ng/mL) of serum GH concentration at each time point.

(range 0.1 to 19.1 ng/mL), respectively. After administration of apomorphine, mean serum GH concentrations at 30 minutes (G3) and 60 minutes (G4) were 13.4 ng/mL (range 0.1 to 53.8 ng/mL) and 11.9 ng/mL (range 2.1 to 37.0 ng/mL), respectively (Table 3). The increase in serum GH concentration following apomorphine was significantly greater than following saline ($P = 0.008$, paired samples *t*-test).

Tolerability and Dosage of Apomorphine

All research participants whose PET data were used in this analysis completed the protocol without any adverse events ($n = 12$). During the course of the study, one participant could not complete the protocol owing to bradycardia and hypotension immediately after the administration of apomorphine (20 μg/kg subcutaneous). This participant responded well to intravenous hydration with a restoration of vital signs to baseline and was discharged home without any residual side effects. In the light of this adverse event, we sought approval from the Institutional Review Board to perform subsequent PET studies with a lower dose of apomorphine (10 μg/kg subcutaneous; $n = 8$). We confirmed that there were no significant differences in the magnitude of serum GH increase in response to apomorphine between individuals receiving the higher relative to lower dose (independent samples *t*-test). Therefore, the results presented above include data from these subjects, as well as from the four participants who were previously studied after injection of 20 μg/kg subcutaneous apomorphine.

Discussion

We have developed a novel PET method using ^{11}C-labeled AA and have used it for the first time in humans to visualize *in vivo* dopaminergic neurotransmission in the resting state. Consistent with our expectation based on animal studies (Bhattacharjee *et al*, 2008*b*), we observed measurable increases in the incorporation coefficient K* for AA in response to apomorphine in several brain regions. While interpreting the regional distribution of changes in K*, we believe that the increases and decreases in incorporation of AA reflect neuronal signaling events downstream of the activated D_2 receptors that are coupled to $cPLA_2$ (Bhattacharjee *et al*, 2005; Vial and Piomelli, 1995). These changes likely reflect consequences of direct D_2 activation and of dopaminergic modulation of other neurotransmitter circuits such as those including glutamatergic and histaminergic synapses (Esposito *et al*, 2007). Consistent with this hypothesis, studies have shown that glutamate acting at *N*-methyl-D-aspartate receptors evokes AA release from different neuronal cell types (Dumuis *et al*, 1988; Lazarewicz *et al*, 1988; Sanfeliu *et al*, 1990) and in the intact rat brain (Basselin *et al*, 2006). Conversely, it has been shown that dopamine can excite histamine neurons through D_2 receptor activation (Haas *et al*, 2008; Traiffort *et al*, 1992). Consistent with these observations, in a previous study in rats that examined the brain AA signal after D_2-like receptor activation by apomorphine, we suggested that changes in K* reflect direct and indirect downstream effects in circuits containing D_2-like receptors or other types of $cPLA_2$-coupled receptors, such as NMDA, serotonergic 5-$HT_{2A/2C}$, and cholinergic muscarinic $M_{1,3,5}$ receptors (Basselin *et al*, 2005, 2006; Bayon *et al*, 1997; DeGeorge *et al*, 1991; Felder *et al*, 1990). Another important consideration in the interpretation of regional changes in K* is the possible opposing effects of D_1 and D_2 receptor stimulation on $cPLA_2$-mediated release of AA. It has been shown that although D_2 receptor activation potentiates AA release induced by the calcium ionophore A23187 or the purinergic agonist ATP, D_1 receptor stimulation has the opposite effect (Schinelli *et al*, 1994).

Although our current results represent a substantial extension of our previous preclinical observations in unanesthetized rodents, the magnitude of apomorphine-induced increases in K* that we observed in this human study is considerably lower than those in animal experiments (Bhattacharjee *et al*, 2008*b*). The most likely explanation for these differences is the different doses of apomorphine administered in animal relative to human studies. We injected 0.5 mg/kg of apomorphine intraperitoneally in rodent experiments, whereas in the current human volunteer study, the dose of apomorphine that we determined could be safely administered was 10 to 20 μg/kg subcutaneous. The considerably higher dose of apomorphine challenge used in animal studies likely resulted in a much better signal:noise ratio than in this human study. This is an important consideration that must be taken into account in the interpretation of our current results. The dose-limiting considerations in the use of apomorphine as a

pharmacological challenge in healthy human subjects may thus also limit our ability to derive accurate quantitative estimates of D_2 receptor-mediated AA release in the paradigm we used in these studies.

Our findings of increases in rCBF in response to apomorphine are consistent with previous [^{15}O]water PET investigations (Kapur *et al*, 1994; Grasby *et al*, 1993). Although the regional pattern of changes in rCBF after apomorphine were distinct from those in K* in most regions, suggesting that these were associated with altered activity of neurons not involving $cPLA_2$ activation, we observed concomitant increases in K* and rCBF in the right fusiform gyrus, suggesting a close coupling of neuronal activity and $cPLA_2$-initiated signal transduction in this brain region. However, this coupling does not reflect the effect of altered rCBF on K* for AA, since K* has been shown to be blood flow independent (Chang *et al*, 1997; Esposito *et al*, 2008). Our findings are also comparable to a previous fluorodeoxyglucose PET study that showed increased glucose metabolism in the posterior frontal and inferior parietal regions after apomorphine (Cleghorn *et al*, 1991).

Consistent with previous studies, we did not observe any significant change in rCBF in the striatum (Grasby *et al*, 1993; Kapur *et al*, 1994). Similarly, no change in K* was seen in this region, which has a very high density of dopamine receptors. To explain this apparent paradox, Kapur *et al*, (1994) have suggested that although receptor-binding studies pinpoint regions with high receptor density (Farde *et al*, 1986; Sedvall *et al*, 1986; Sedvall, 1990), studies identifying functional effects of dopaminergic drugs, such as ours, map the regions where receptor binding in such regions leads to downstream functional effects. Therefore, it is plausible that activation of D_1/D_2 receptors at striatal sites produces modulated neuronal firing and $cPLA_2$-mediated AA release in the extrastriatal brain regions identified in our study. Supporting this idea, our observed increases in K* occurred in regions receiving rich projections from the striatum, including the motor cortex and mesial frontal cortex (Alexander and Crutcher, 1990). We also found predominantly right hemispheric increases in K* after apomorphine. Although our study sample included both right- and left-handed individuals, this observation is consistent with the reported hemispheric asymmetry within the dopaminergic system in healthy individuals (Cannon *et al*, 2009; Tomer *et al*, 2008; Vernaleken *et al*, 2007).

Besides the single subject who experienced bradycardia and hypotension after 20 μg/kg subcutaneous apomorphine, and who responded to intravenous hydration, no serious adverse events were observed in response to apomorphine at the doses used in this study (10 to 20 μg/kg subcutaneous). Previous studies have reported minor side effects including somnolence, nausea, dizziness, and hallucinations in response to apomorphine (Aymard *et al*, 2003; Bowron, 2004; Menon and Stacy, 2007). To prevent apomorphine-induced nausea during the PET protocol, we premedicated study participants with the antiemetic trimethobenzamide (Bowron, 2004). This medication was well tolerated without any side effects and completely prevented nausea during the course of the scanning procedure.

To confirm a robust central response to apomorphine, we assayed serum concentration of GH at baseline and at 30 and 60 minutes after injection of saline vehicle and apomorphine. Consistent with previous reports, we observed significant increases in serum GH levels in response to apomorphine relative to saline vehicle (Aymard *et al*, 2003; Kapur *et al*, 1994). Therefore, this finding suggests that the changes in K* and rCBF observed after apomorphine were induced by a measurable central effect of the drug.

Some important differences between this investigation and previous PET studies of dopaminergic neurotransmission merit consideration in interpreting our results. Unlike other studies, we did not include a cognitive task in our PET paradigm (Grasby *et al*, 1993; Kapur *et al*, 1994), choosing instead to measure the PET signals in a true resting state. Cognitive tasks have been used in previous PET studies of dopaminergic function to standardize the behavioral state and thereby reduce intrasubject and intersubject variability in rCBF. However, we chose not to use a cognitive task in our PET protocol, to avoid task-induced activations of brain regions that might in turn influence changes in K* and rCBF. However, this may have reduced the signal:noise ratio of our observations by increasing the baseline variance in neuronal activity. Another factor to be considered is that, in the interests of subject safety and to prevent apomorphine-induced nausea, we premedicated our study participants with trimethobenzamide. There is some suggestion that benzamides possess presynaptic and postsynaptic actions on dopaminergic systems (Elliott *et al*, 1977). It is unclear to what extent this medication may have influenced our PET results. An additional caveat that must be considered in the interpretation of our findings is that with the relatively small number ($N=12$) of subjects, our PET results reported at a significance threshold of $P<0.005$ and a spatial extent >20 voxels, are uncorrected for multiple comparisons. Given that this was an exploratory analysis, and our principal aim was to evaluate the feasibility of the [1-^{11}C]AA PET method to study brain dopaminergic function, we chose to present all observed regional differences without correction for multiple hypotheses testing. Although this may have increased the risk of type-I error, we believe that our approach now allows for further directed analyses of changes in specific brain regions and testing *a priori* hypotheses on dopaminergic function in health and disease states.

In summary, we used [1-^{11}C]arachidonate PET in a study of healthy human subjects to show measurable effects on regional brain AA incorporation and rCBF in response to pharmacological challenge with apomorphine, a D_1/D_2 receptor agonist. Our study

shows the feasibility of this strategy to visualize *in vivo* signal transduction events accompanying dopaminergic neurotransmission. Future studies testing the utility of this method in studying perturbations in brain dopaminergic function in disease states such as Parkinson's disease and schizophrenia are warranted.

Acknowledgements

MT and SIR are grateful to Ms Jane Bell (deceased) for her invaluable contributions to this study. We also acknowledge the dedication and professionalism of the nursing staff of the 7SE Unit, NIH Clinical Center.

Disclosure/conflict of interest

The authors declare no conflict of interest.

References

Alexander GE, Crutcher MD (1990) Functional architecture of basal ganglia circuits: neural substrates of parallel processing. *Trends Neurosci* 13:266–71

Aymard G, Berlin I, de Brettes B, Diquet B (2003) Pharmacokinetic-pharmacodynamic study of apomorphine's effect on growth hormone secretion in healthy subjects. *Fundam Clin Pharmacol* 17:473–81

Basselin M, Chang L, Bell JM, Rapoport SI (2006) Chronic lithium chloride administration attenuates brain NMDA receptor-initiated signaling via arachidonic acid in unanesthetized rats. *Neuropsychopharmacology* 31:1659–74

Basselin M, Chang L, Seemann R, Bell JM, Rapoport SI (2005) Chronic lithium administration to rats selectively modifies 5-HT2A/2C receptor-mediated brain signaling via arachidonic acid. *Neuropsychopharmacology* 30: 461–72

Bayon Y, Hernandez M, Alonso A, Nunez L, Garcia-Sancho J, Leslie C, Sanchez Crespo M, Nieto ML (1997) Cytosolic phospholipase A2 is coupled to muscarinic receptors in the human astrocytoma cell line 1321N1: characterization of the transducing mechanism. *Biochem J* 323(Pt 1):281–7

Bhattacharjee AK, Chang L, Chen M, White L, Bell JM, Bazinet RP, Rapoport SI (2008a) Chronic d-amphetamine depresses an imaging marker of arachidonic acid metabolism in rat brain. *Int J Neuropsychopharmacol* 11:957–69

Bhattacharjee AK, Chang L, Lee HJ, Bazinet RP, Seemann R, Rapoport SI (2005) D-2 but not D-1 dopamine receptor stimulation augments brain signaling involving arachidonic acid in unanesthetized rats. *Psychopharmacology* 180:735–42

Bhattacharjee AK, Chang L, White L, Bazinet RP, Rapoport SI (2006) D-Amphetamine stimulates D-2 dopamine receptor-mediated brain signaling involving arachidonic acid in unanesthetized rats. *J Cereb Blood Flow Metab* 26:1378–88

Bhattacharjee AK, Chang L, White L, Bazinet RP, Rapoport SI (2008b) Imaging apomorphine stimulation of brain arachidonic acid signaling via D2-like receptors in unanesthetized rats. *Psychopharmacology (Berl)* 197: 557–66

Bhattacharjee AK, Meister LM, Chang L, Bazinet RP, White L, Rapoport SI (2007) *In vivo* imaging of disturbed pre- and post-synaptic dopaminergic signaling via arachidonic acid in a rat model of Parkinson's disease. *Neuroimage* 37:1112–21

Bowron A (2004) Practical considerations in the use of apomorphine injectable. *Neurology* 62:S32–6

Brooks DJ, Lammertsma AA, Beaney RP, Leenders KL, Buckingham PD, Marshall J, Jones T (1984) Measurement of regional cerebral pH in human subjects using continuous inhalation of 11CO2 and positron emission tomography. *J Cereb Blood Flow Metab* 4:458–65

Brooks DJ, Piccini P (2006) Imaging in Parkinson's disease: the role of monoamines in behavior. *Biol Psychiatry* 59:908–18

Cannon DM, Klaver JM, Peck SA, Rallis-Voak D, Erickson K, Drevets WC (2009) Dopamine type-1 receptor binding in major depressive disorder assessed using positron emission tomography and [C-11]NNC-112. *Neuropsychopharmacology* 34:1277–87

Chang MC, Arai T, Freed LM, Wakabayashi S, Channing MA, Dunn BB, Der MG, Bell JM, Sasaki T, Herscovitch P, Eckelman WC, Rapoport SI (1997) Brain incorporation of [1-11C]arachidonate in normocapnic and hypercapnic monkeys, measured with positron emission tomography. *Brain Res* 755:74–83

Channing MA, Freed L, Wakabayashi S, Carson R, Simpson N, Dunn BB, Rapoport SI (1992) [1-11C]labeled polyhomoallyilic fatty acids: phospholipid metabolic tracers for the brain. *Am J Nuclear Med* 13:1093

Clark JD, Lin LL, Kriz RW, Ramesha CS, Sultzman LA, Lin AY, Milona N, Knopf JL (1991) A novel arachidonic acid-selective cytosolic PLA_2 contains a $Ca^{(2+)}$-dependent translocation domain with homology to PKC and GAP. *Cell* 65:1043–51

Cleghorn JM, Szechtman H, Garnett ES, Nahmias C, Brown GM, Kaplan RD, Szechtman B, Franco S (1991) Apomorphine effects on brain metabolism in neuroleptic-naive schizophrenic patients. *Psychiatry Res* 40:135–53

Cropley VL, Fujita M, Innis RB, Nathan PJ (2006) Molecular imaging of the dopaminergic system and its association with human cognitive function. *Biol Psychiatry* 59:898–907

DeGeorge JJ, Nariai T, Yamazaki S, Williams WM, Rapoport SI (1991) Arecoline-stimulated brain incorporation of intravenously administered fatty acids in unanesthetized rats. *J Neurochem* 56:352–5

Dolan RJ, Fletcher P, Frith CD, Friston KJ, Frackowiak RS, Grasby PM (1995) Dopaminergic modulation of impaired cognitive activation in the anterior cingulate cortex in schizophrenia. *Nature* 378:180–2

Dumuis A, Sebben M, Haynes L, Pin JP, Bockaert J (1988) NMDA receptors activate the arachidonic acid cascade system in striatal neurons. *Nature* 336:68–70

Elliott PN, Jenner P, Huizing G, Marsden CD, Miller R (1977) Substituted benzamides as cerebral dopamine antagonists in rodents. *Neuropharmacology* 16: 333–42

Elsinga PH, Hatano K, Ishiwata K (2006) PET tracers for imaging of the dopaminergic system. *Curr Med Chem* 13:2139–53

Esposito G, Giovacchini G, Der M, Liow JS, Bhattacharjee AK, Ma K, Herscovitch P, Channing M, Eckelman WC, Hallett M, Carson RE, Rapoport SI (2007) Imaging signal transduction via arachidonic acid in the human brain during visual stimulation, by means of positron emission tomography. *Neuroimage* 34:1342–51

Esposito G, Giovacchini G, Liow JS, Bhattacharjee AK, Greenstein D, Schapiro M, Hallett M, Herscovitch P, Eckelman WC, Carson RE, Rapoport SI (2008) Imaging neuroinflammation in Alzheimer's disease with radiolabeled arachidonic acid and PET. *J Nucl Med* 49: 1414–21

Farde L, Hall H, Ehrin E, Sedvall G (1986) Quantitative analysis of D2 dopamine receptor binding in the living human brain by PET. *Science* 231:258–61

Felder CC, Kanterman RY, Ma AL, Axelrod J (1990) Serotonin stimulates phospholipase A2 and the release of arachidonic acid in hippocampal neurons by a type 2 serotonin receptor that is independent of inositol phospholipid hydrolysis. *Proc Natl Acad Sci USA* 87:2187–91

Giovacchini G, Chang MC, Channing MA, Toczek M, Mason A, Bokde AL, Connolly C, Vuong BK, Ma Y, Der MG, Doudet DJ, Herscovitch P, Eckelman WC, Rapoport SI, Carson RE (2002) Brain incorporation of [11C]arachidonic acid in young healthy humans measured with positron emission tomography. *J Cereb Blood Flow Metab* 22:1453–62

Giovacchini G, Lerner A, Toczek MT, Fraser C, Ma K, DeMar JC, Herscovitch P, Eckelman WC, Rapoport SI, Carson RE (2004) Brain incorporation of 11C-arachidonic acid, blood volume, and blood flow in healthy aging: a study with partial-volume correction. *J Nucl Med* 45:1471–9

Grasby PM, Friston KJ, Bench CJ, Cowen PJ, Frith CD, Liddle PF, Frackowiak RS, Dolan RJ (1993) The effect of the dopamine agonist, apomorphine, on regional cerebral blood flow in normal volunteers. *Psychol Med* 23:605–12

Haas HL, Sergeeva OA, Selbach O (2008) Histamine in the nervous system. *Physiol Rev* 88:1183–241

Hayakawa T, Chang MC, Bell JM, Seeman R, Rapoport SI, Appel NM (1998) Fatty acid incorporation depicts brain activity in a rat model of Parkinson's disease. *Brain Res* 807:177–81

Hayakawa T, Chang MC, Rapoport SI, Appel NM (2001) Selective dopamine receptor stimulation differentially affects [3H]arachidonic acid incorporation, a surrogate marker for phospholipase A2-mediated neurotransmitter signal transduction, in a rodent model of Parkinson's disease. *J Pharmacol Exp Ther* 296:1074–84

Herscovitch P, Markham J, Raichle ME (1983) Brain blood flow measured with intravenous O-15 water: I. Theory and error analysis. *J Nuclear Med* 24:782–9

Hirvonen J, Hietala J (2011) Dysfunctional brain networks and genetic risk for schizophrenia: specific neurotransmitter systems. *CNS Neurosci Ther* 17:89–96

Ibanez V, Pietrini P, Alexander GE, Furey ML, Teichberg D, Rajapakse JC, Rapoport SI, Schapiro MB, Horwitz B (1998) Regional glucose metabolic abnormalities are not the result of atrophy in Alzheimer's disease. *Neurology* 50:1585–93

Jenkinson M, Smith S (2001) A global optimisation method for robust affine registration of brain images. *Med Image Anal* 5:143–56

Kapur S, Meyer J, Wilson AA, Houle S, Brown GM (1994) Activation of specific cortical regions by apomorphine: an [15O]H2O PET study in humans. *Neurosci Lett* 176:21–4

Lazarewicz JW, Wroblewski JT, Palmer ME, Costa E (1988) Activation of N-methyl-D-aspartate-sensitive glutamate receptors stimulates arachidonic acid release in primary cultures of cerebellar granule cells. *Neuropharmacology* 27:765–9

Menon R, Stacy M (2007) Apomorphine in the treatment of Parkinson's disease. *Expert Opin Pharmacother* 8:1941–50

Muller-Gartner HW, Links JM, Prince JL, Bryan RN, McVeigh E, Leal JP, Davatzikos C, Frost JJ (1992) Measurement of radiotracer concentration in brain gray matter using positron emission tomography: MRI-based correction for partial volume effects. *J Cereb Blood Flow Metab* 12:571–83

Nikolaus S, Antke C, Kley K, Poeppel TD, Hautzel H, Schmidt D, Muller HW (2007) Investigating the dopaminergic synapse *in vivo*. I. Molecular imaging studies in humans. *Rev Neurosci* 18:439–72

Nilsson CL, Hellstrand M, Ekman A, Eriksson E (1998) Direct dopamine D^2-receptor-mediated modulation of arachidonic acid release in transfected CHO cells without the concomitant administration of a Ca^{2+}-mobilizing agent. *Br J Pharmacol* 124:1651–8

Rapoport SI (2001) *In vivo* fatty acid incorporation into brain phosholipids in relation to plasma availability, signal transduction and membrane remodeling. *J Mol Neurosci* 16:243–61; discussion 79–84

Rapoport SI (2003) *In vivo* approaches to quantifying and imaging brain arachidonic and docosahexaenoic acid metabolism. *J Pediatr* 143:S26–34

Robinson PJ, Noronha J, DeGeorge JJ, Freed LM, Nariai T, Rapoport SI (1992) A quantitative method for measuring regional *in vivo* fatty-acid incorporation into and turnover within brain phospholipids: review and critical analysis. *Brain Res Brain Res Rev* 17:187–214

Sanfeliu C, Hunt A, Patel AJ (1990) Exposure to N-methyl-D-aspartate increases release of arachidonic acid in primary cultures of rat hippocampal neurons and not in astrocytes. *Brain Res* 526:241–8

Scarselli M, Armogida M, Pardini C, Chiacchio S, Corsini GU (2001) Apomorphine. A novel effect for an old compound. *Adv Neurol* 86:367–72

Schinelli S, Paolillo M, Corona GL (1994) Opposing actions of D1- and D2-dopamine receptors on arachidonic acid release and cyclic AMP production in striatal neurons. *J Neurochem* 62:944–9

Sedvall G (1990) PET imaging of dopamine receptors in human basal ganglia: relevance to mental illness. *Trends Neurosci* 13:302–8

Sedvall G, Farde L, Stone-Elander S, Halldin C (1986) Dopamine D1-receptor binding in the living human brain. *Adv Exp Med Biol* 204:119–24

Tomer R, Goldstein RZ, Wang GJ, Wong C, Volkow ND (2008) Incentive motivation is associated with striatal dopamine asymmetry. *Biol Psychol* 77:98–101

Traiffort E, Ruat M, Arrang JM, Leurs R, Piomelli D, Schwartz JC (1992) Expression of a cloned rat histamine H2 receptor mediating inhibition of arachidonate release and activation of cAMP accumulation. *Proc Natl Acad Sci USA* 89:2649–53

Vernaleken I, Weibrich C, Siessmeier T, Buchholz HG, Rosch F, Heinz A, Cumming P, Stoeter P, Bartenstein P, Grunder G (2007) Asymmetry in dopamine D-2/3 receptors of caudate nucleus is lost with age. *Neuroimage* 34:870–8

Vial D, Piomelli D (1995) Dopamine D_2 receptors potentiate arachidonate release via activation of cytosolic, arachidonate-specific phospholipase A_2. *J Neurochem* 64:2765–72

Volkow ND, Fowler JS, Wang GJ, Baler R, Telang F (2009) Imaging dopamine's role in drug abuse and addiction. *Neuropharmacology* 56(Suppl 1):3–8